

**Studies of Thermally Unstable Accretion Disks around Black Holes
with Adaptive Pseudospectral Domain Decomposition Method.
II. Limit-Cycle Behavior in accretion disks around Kerr black holes**

Li Xue*, Aleksander Sądowski[†], Marek A. Abramowicz^{‡,†} and Ju-Fu Lu*

Received _____; accepted _____

*Department of Physics and Institute of Theoretical Physics and Astrophysics, Xiamen University, Xiamen, Fujian 361005, China; lixue@xmu.edu.cn, lujf@xmu.edu.cn

[†]Nicolaus Copernicus Astronomical Center, Bartycka 18, 00-716 Warszawa, Poland

[‡]Department of Physics, Göteborg University, SE-412-96 Göteborg, Sweden

ABSTRACT

For the first time ever, we derive equations governing the time-evolution of fully relativistic slim accretion disks in the Kerr metric, and numerically construct their detailed non-stationary models. We discuss applications of these general results to a possible limit-cycle behavior of thermally unstable disks. Our equations and numerical method are applicable in a wide class of possible viscosity prescriptions, but in this paper we use a diffusive form of the “standard alpha prescription” that assumes the viscous torque is proportional to the total pressure. In this particular case, we find that the parameters which dominate the limit-cycle properties are the mass-supply rate and the value of the alpha-viscosity parameter. Although the duration of the cycle (or the outburst) does not exhibit any clear dependence on the black hole spin, the maximal outburst luminosity (in the Eddington units) is positively correlated with the spin value. We suggest a simple method for a rough estimate of the black hole spin based on the maximal luminosity and the ratio of outburst to cycle durations. We also discuss a temperature-luminosity relation for the Kerr black hole accretion discs limit-cycle. Based on these results we discuss the limit-cycle behavior observed in microquasar GRS 1915+105. We also extend this study to several non-standard viscosity prescriptions, including a “delayed heating” prescription recently stimulated by the recent MHD simulations of accretion disks.

Subject headings: accretion, accretion disks — black hole physics — hydrodynamics — instabilities

1. Introduction

This work is motivated by the fundamental issue of how to find the proper viscosity prescription in the black hole (BH) accretion disk theory. The “standard alpha-prescription”, introduced in the seminal paper by Shakura & Sunyaev (1973), assumes that the viscous torque \mathbb{T} is proportional to the total pressure P ,

$$\mathbb{T} = -\alpha P, \tag{1}$$

where the dimensionless “viscosity coefficient” $0 \leq \alpha \leq 1$ is a universal phenomenological constant. Hydrodynamical accretion disk models constructed with the help of the above formula are remarkably successful in describing observed properties of real disks, but only when these disks are *stationary* and *not very luminous*, i.e. when

$$\frac{\partial}{\partial t} = 0 \quad \text{and} \quad L < 0.3 L_{\text{Edd}}. \tag{2}$$

This is not a surprise. An extension of the Shakura-Sunyaev theory in terms of the “slim disk” models (Abramowicz et al. 1988), *predicted* that the properties of accretion disks weakly depend on α *only* in the range (2). Outside this range, the predicted observables strongly depend on the form of the viscosity prescription and on the assumed value of α : the “small-alpha disks”, $\alpha \approx 0.01$, are remarkably different from the “moderate-alpha disks”, $\alpha \approx 0.1$. For luminosities higher than $0.3 L_{\text{Edd}}$ the dependence on α is convoluted with the details of radiative transfer, vertical structure, and general relativistic effects inside and outside the disk. In addition, the relativistic effects strongly depend on the BH spin.

These severe technical complications sometimes mask a fundamental problem. On one hand, with the help of hydrodynamical models we are able to accurately calculate observable properties of accretion disks, but only if we assume (1) or other ad hoc formula for the stress. However, outside the range of applicability (2), this approach is questionable and most probably wrong. On the other hand, the MHD simulations which calculate \mathbb{T}

from the first principles, are not sufficiently realistic today in treating radiative transfer and other relevant physics accurately enough to calculate realistic observable properties of accretion disks.

One possible way to make progress is to calculate “the state-of-art” hydrodynamical models with radiative transfer, vertical structure, general relativistic effects, etc. treated as accurately as possible and with a properly chosen “MHD viscosity prescription” motivated directly by the MHD simulations. Some phenomenological parameters that may appear in the MHD prescription, should be then fixed by a detailed comparison with observations. This principle was recently used by Sądowski (2009) and Sądowski et al. (2010) who calculated a network of models of *stationary* slim accretion disks, covering a wide range of the relevant parameter space. Our present work depends on these models in several important aspects. In particular, it takes the stationary models calculated by Sądowski as the initial condition for the non-stationary calculations.

We also borrow heavily from the previous paper of our long-term research program (Li et al. 2007, hereafter Paper I). We have introduced there the *adaptive pseudospectral domain decomposition* method, which we also use in the present paper. Results of Li et al. (2007) have been in a good agreement with the studies on the limit-cycle behavior in the radiation-pressure supported slim disks by Szuszkiewicz & Miller (2001, hereafter SM01). These, and all other previous numerical studies of the subject (Honma et al. 1991; Lasota and Pelat 1991; Szuszkiewicz & Miller 1997, 1998, 2001; Teresi et al. 2004a,b; Mayer & Pringle 2006), have been performed within the Newtonian hydrodynamics, in which the Newtonian gravitational potential is replaced by the Paczyński pseudo-Newtonian potential introduced by Paczyński & Wiita (1980). It reasonably models gravity of non-rotating black holes, but fails in the case of rapidly rotating ones.

Our present paper extends these previous studies by making three new developments:

(i) We perform the first ever fully relativistic *time-dependent* numerical study for a limit-cycle in black hole accretion disks. (ii) We provide a theoretical tool for understanding some observational aspects of GRS 1915+105 (and possibly similar sources) which are unique in showing *both* the evidence for a near-extreme black hole spin, *and* the limit-cycle behavior. (iii) We investigate the possibility of using the observed properties of the limit cycle to estimate the black hole spin. These issues are relevant for studying the fundamental issue of the viscosity prescription.

2. Basic equations

In this paper, we consider the axisymmetric relativistic accretion flows around Kerr BHs. We use the Boyer-Lindquist spherical coordinates t, r, θ, ϕ to describe the space-time around a BH. Putting all of the complicated derivations into Appendix A, the basic equations which govern the dynamical behavior of accretion flows can be written as following*.

- Mass conservation:

$$\frac{\partial \Sigma}{\partial t} = -\frac{r\Delta^{1/2}}{\gamma A^{1/2}} \left[\Sigma \frac{\partial u^t}{\partial t} + \frac{1}{r} \frac{\partial}{\partial r} \left(r \Sigma \frac{V}{\sqrt{1-V^2}} \frac{\Delta^{1/2}}{r} \right) \right], \quad (3)$$

where Σ ($= 2H\rho$) is the surface density with H being the half thickness and ρ being the mass density, V is the radial velocity measured in the corotating frame (CRF), γ is the Lorentz factor, $\Delta = r^2 - 2Mr + a^2$ and $A = r^4 + r^2a^2 + 2Mra^2$ with M and a being the BH mass and spin per unit mass, respectively. The derivative of the contravariant t -component of the four-velocity $\frac{\partial u^t}{\partial t}$ is defined in equation (A14) as a function of $\frac{\partial V}{\partial t}$ and $\frac{\partial \mathcal{L}}{\partial t}$ (see the following equations (4) and (5) for the definitions of

*Throughout this paper we use the $c = G = 1$ units.

these two derivatives).

- Radial momentum conservation:

$$\frac{\partial V}{\partial t} = \frac{\sqrt{1-V^2}\Delta}{\gamma A^{1/2}} \left[-\frac{V}{1-V^2} \frac{\partial V}{\partial r} + \frac{\mathcal{A}}{r} - \frac{1-V^2}{\rho} \frac{\partial p}{\partial r} \right], \quad (4)$$

where \mathcal{A} is defined in equation (A19a), p ($= \frac{k_B}{\mu m_p} \rho T + p_{\text{rad}}$) is the total pressure consisting of the gas and radiation pressure.

- Angular momentum conservation:

$$\frac{\partial \mathcal{L}}{\partial t} = -\frac{V\Delta}{\gamma\sqrt{1-V^2}A^{1/2}} \frac{\partial \mathcal{L}}{\partial r} + \frac{\Delta^{1/2}}{\gamma\Sigma A^{1/2}} \frac{\partial}{\partial r} \left(\frac{\nu\Sigma A^{3/2}\Delta^{1/2}\gamma^3}{r^4} \frac{\partial \Omega}{\partial r} \right), \quad (5)$$

where $\mathcal{L}(=u_\phi)$ is the angular momentum per unit mass, Ω is the angular velocity with respect to the stationary observer (see equation (A19b) for its definition), and ν is the kinematic viscosity coefficient. We evaluate ν with a diffusive form of the “standard alpha prescription” (equation (1)),

$$\nu = \frac{2}{3}\alpha H \sqrt{\frac{p}{\rho}}. \quad (6)$$

- Half thickness evolution:

$$\frac{\partial H}{\partial t} = -U \cos \Theta_H - \frac{1}{\gamma} \frac{V}{\sqrt{1-V^2}} \frac{\partial H}{\partial r}, \quad (7)$$

where H is the half thickness of the disk, U is the vertical velocity, and Θ_H ($= \arccos \frac{H}{r}$) is the colatitude angle corresponding to the disk surface.

- Surface vertical motion:

$$\frac{\partial U}{\partial t} = \frac{\Delta^{1/2}}{\gamma^2 A^{1/2} \cos \Theta_H} \mathcal{R} - \frac{U}{\gamma^2} \left(\frac{V}{(1-V^2)^2} \frac{\partial V}{\partial t} + \frac{\mathcal{L}r^2}{A} \frac{\partial \mathcal{L}}{\partial t} \right) - \frac{U}{H} \frac{\partial H}{\partial t}, \quad (8)$$

where \mathcal{R} is defined in equation (A33a). Equations (7) and (8) describe the evolution of the disk surface. This kind of vertical treatment was first introduced

by Szuszkiewicz & Miller (2001) in order to mimic some advantageous features of a two-dimensional model in a one-dimensional (see Papaloizou & Szuszkiewicz 1994) study. Thus, our study also exhibits some two-dimensional features (e.g., the vertical component of the velocity at the disk surface) so that we prefer to call it 1.5-dimensional.

- Energy conservation:

$$\frac{\partial T}{\partial t} = \frac{1}{\Sigma} \frac{r \Delta^{1/2}}{\gamma A^{1/2}} \left[\frac{F^+ - F^-}{c_V} + (\Gamma_3 - 1) T \Sigma \left(-\frac{\partial u^t}{\partial t} - \frac{1}{r^2} \frac{\partial}{\partial r} (r^2 u^r) \right) \right] - \frac{V \Delta}{\gamma \sqrt{1 - V^2} A^{1/2}} \frac{\partial T}{\partial r}, \quad (9)$$

where T is the temperature of gas, F^+ is the local viscous heat generation rate (equation (A37)), and F^- is the radiative cooling rate given by the bridge formulae, which is valid for both optically thick and thin regimes,

$$F^- = \frac{8\sigma T^4}{3\tau_R/2 + \sqrt{3} + 1/\tau_P}, \quad (10)$$

where τ_R and τ_P are the Rosseland and Planck mean optical depths (see e.g., Abramowicz et al. 1996). The corresponding radiation pressure is given by,

$$p_{\text{rad}} = \frac{F^-}{2} \left(\tau_R + \frac{2}{\sqrt{3}} \right). \quad (11)$$

c_V and Γ_3 are defined in equations (A43a) and (A43b), respectively.

In this paper, the properties of an accretion disk depend on three crucial parameters:

- Dimensionless black hole spin a^* :

$$a^* \equiv \frac{a}{GM/c} = \frac{a}{M}, \quad -1 \leq a^* < 1; \quad (12)$$

- Diffusive viscosity parameter α (see equation (6)):

$$0 < \alpha < 1;$$

- Dimensionless mass-supply rate \dot{m} :

$$\dot{m} \equiv \frac{\dot{M}(r_{\text{out}})}{\dot{M}_{\text{Edd}}}. \quad (13)$$

Where $\dot{M}(r_{\text{out}})$ and $\dot{M}_{\text{Edd}} \equiv 64\pi GM/(c\kappa_{\text{es}})$ are the accretion rate at the outer boundary $r = r_{\text{out}}$ and the Eddington accretion rate (corresponding to the Eddington luminosity for a non-rotating BH), respectively.

3. Numerical method

Following Paper I, we use *the adaptive pseudospectral domain decomposition method* to solve the basic equations. This method has already been validated by the successful reproduction of the limit-cycle behavior in the pseudo-Newtonian framework. The relativistic time-dependent code used in this work is an upgraded version of the previous pseudo-Newtonian one. For the initial conditions, we interpolate the relativistic stationary global slim disk solution of Sądowski (2009) on the grid of the time-dependent code. We study the accretion disk around a BH with mass $M = 10M_{\odot}$ and setup the computation domain from a radius between the BH horizon and ISCO (Innermost Stable Circular Orbit), say $r = 2.5r_g$ for a nonrotating BH ($r_{\text{ISCO}} = 3r_g$), to 10^3r_g ($r_g = 2GM/c^2 = 2M$). As in Paper I, the computational domain includes a highly supersonic region, with high radial velocities (about $0.2 \sim 0.3c$ at the inner boundary). At this inner boundary, we adopt the free-type boundary conditions, i.e., we let all variables evolve naturally according to their basic equations except \mathcal{L} , which is set by an extrapolation of the nearest two points. This kind of inner boundary conditions, in practice, are quite stable because the accretion flow always supersonically inflows beyond the inner boundary without numerical spurious reflection. Meanwhile, they are also more natural and physical than directly setting the viscous torque to vanish outside the BH's horizon. At the outer boundary, we fix V and

Σ to ensure constant mass supply, and also fix \mathcal{L} and set $U = 0$ to avoid the numerical spurious evolution.

We have performed computations for two particular cases to check the relativistic code. Both consist of an accretion disk with $\alpha = 0.07$ and $\dot{m} = 0.02$, while the BH spin was set to $a^* = 0$ and $a^* = 0.95$, respectively. The essential difference between these two cases is in the thermal stability. According the local analysis of stability (e.g., Kato et al. 1998, p.155), only the non-spinning case is thermally stable (see Fig. 1). In Figure 2, we show the profiles of surface density and temperature for both cases. It is clear that for the $a^* = 0$ case (left panel), the disk remains in the steady state for more than 1.2×10^4 seconds, therefore it can be regarded as a stable disk (the tiny differences between the initial state and the snapshot are due to the differences of numerical methods used for obtaining stationary and time-dependent solutions and are considered not significant). On the contrary, for the highly spinning case (right panel) the disk undergoes an outburst immediately after the beginning of simulation. These results validate the ability of the code to distinguish the thermally stable and unstable behavior, and also prove that the BH spin significantly influences the thermal stability of the accretion disk, which motivates us to explore the limit-cycle behavior of thermally unstable disks around Kerr BHs.

4. Numerical exploration

4.1. Parameter space and characteristic quantities

In order to understand the effects of BH spin on the limit-cycle behavior, it is necessary to investigate the parameter space (a^*, α, \dot{m}) with a series of models. In this section, we describe and discuss results of twelve runs assuming different sets of the input parameters span on the grid: $a^* = (0, 0.5, 0.95)$, $\alpha = (0.07, 0.1)$, and $\dot{m} = (0.06, 0.1)$ (cf. Table 1). All

of the cases are thermally unstable and undergo recursive limit-cycle evolution.

To describe the limit-cycle behavior, we define four characteristic quantities, which are the Outburst Duration (the full width at half maximum of light-curve, hereafter OD), Cycle Duration (time interval between two outbursts, hereafter CD), ratio of OD to CD, and Maximal Luminosity (the peak value of the light curve during outburst, hereafter ML; calculated intrinsically, with no ray-tracing), respectively. In Figure 3, we visualize these definitions on a sketched light-curve.

The computations for each one of those twelve cases continue until the CD converges to a constant value. The constancy of CDs implies that the computations has reached a state uniquely determined by the parameters (a^*, α, \dot{m}) , without any impact of the initial conditions. In practice, the required level of convergence is achieved after three or five cycles. We have performed computations for each case for more than seven cycles (some cases reached ten cycles). Our analysis below is based on the last four cycles only.

In Table 1 we list the mean values, standard and relative deviations of each characteristic quantity for our twelve models. These values are calculated based on the retained cycles only. Since the relative deviations (the percentages in the brackets) are all very low, we do not show the error bars for the data points in the subsequent figures.

4.2. Impact of BH spin

In order to reveal the effects of BH spin on limit-cycle behavior, we have divided our twelve models into four groups to reflect the different effects of viscosity and mass supply (i.e., mass accretion rate at the outer boundary). In Figures 4 and 5, the models with $(\alpha = 0.07, \dot{m} = 0.06)$ and different spins are represented by empty stars, while those with $(\alpha = 0.1, \dot{m} = 0.06)$, $(\alpha = 0.07, \dot{m} = 0.1)$, and $(\alpha = 0.1, \dot{m} = 0.1)$ by filled stars, empty

circles, and filled circles, respectively (both are based on the data from Table 1).

In the four panels of Figure 4 we plot OD, CD, OD/CD and ML as a function of a^* . It is clear that there is no distinct and consistent dependence on a^* neither for OD nor CD (panels (a) and (b)). The ratio of OD to CD (panel (c)) is almost independent of a^* for all sets of input parameters. On the contrary, ML exhibits a perfect correlation with a^* (panel (d)), though this relation is still slightly distorted by the impact of α and \dot{m} .

These facts may be easily understood in the framework of the general relativity. The effects of BH spin are restricted to the innermost region of accretion disks. Therefore, the quantity ML, which corresponds mostly to the radiation emerging from the inner part of an accretion disk, must display a strong dependence on a^* . The other quantities (OD, CD and OD/CD) don't have such a strong dependence on a^* as they depend on the disk structure and its evolution at a wide range of radii (from the inner part up to more than $100r_g$), where the effects of viscosity and mass-supply dominates over the effect of BH spin.

4.3. Possibility of estimating the black hole spin with limit-cycle

As has been discussed in the previous section, the effects of BH spin on the quantities OD and CD are easily disturbed by the complex effects of viscosity and mass-supply; while the ratio OD/CD has no discernible dependence on BH spin. Thus, they cannot serve as proper probes of BH spin. Even ML, which has monotonic and positive correlation with a^* , cannot be used directly to estimate the BH spin, because the dependence of ML on BH spin is significantly affected by other factors (see panel (d) of Figure 4).

None of those quantities can be directly used as a probe, but there still exists the possibility of probing the BH spin with them. In fact, we find that the combination of ML and OD/CD can be used to estimate the BH spin. In Figure 5, we show the OD/CD-ML

diagram for all the models. The ratio OD/CD raises with increasing values of α and \dot{m} , and is hardly dependent on a^* (see panel (c) of Figure 4). It is remarkable that the combined effects of viscosity and mass-supply make ML scale almost linearly with the ratio OD/CD. For a given BH spin there is a single straight line reflecting the dependence of ML on OD/CD. These lines do not intercept and have similar slopes. Therefore, the OD/CD-ML diagram may be used for a rough estimation of BH spin if only the limit cycle parameters can be obtained from observational data.

We find that the dependence of ML on OD/CD may be approximated by the following formula

$$\text{ML} / L_{\text{Edd}} = 7.59 \text{ OD/CD} + 0.71 + 7.18 \eta, \quad (14)$$

where η is the efficiency of accretion for a thin disk and is given by

$$\eta = 1 - \sqrt{1 - \frac{2M}{3r_{\text{ms}}}},$$

with r_{ms} being the radius of the marginally stable orbit. In Figure 5 we plot with dashed lines the fits obtained with these formulae for $a^* = 0, 0.5$ and 0.95 . Given the values of ML and OD/CD, one can easily obtain the radius of the marginally stable orbit from Eq. 14, and subsequently the BH spin.

However, there are at least a few limitations for the application of this method. The first one is related to the fact that the OD/CD-ML relation is still subject to a significant dispersion (see Fig. 5). For a given BH spin, the combined impacts of viscosity and accretion rate result in a relation which is only roughly linear.

The second one is related to the modulation of the emitted radiation by the gravitational redshift and focusing effects near the BH (e.g. Cunningham & Bardeen 1973). In our method, the ratio OD/CD is measured in the Boyer-Lindquist (observer's) time, but ML is intrinsic, i.e., it is the integral of local radiation flux in the whole disk. Thus, one

should calculate ML only after calculating the observed disk spectrum, which is subject to the gravitational effects mentioned above. It would be possible by applying ray-tracing techniques (e.g. Fanton et al. 1997) to solve this issue. However, the calculations will be very complicated and out of the scope of our paper. This is because the precise calculation of the emitting spectrum would require knowledge about the intrinsic local emission which cannot be approximated as a perfect black body, especially in effectively optically thin regions. Even so, we can still anticipate that the apparent MLs would be lower than the intrinsic ones (even for the face on case) due to the reduction of the apparent luminosity of disks by the gravitational redshift. However, this decrease should not be strong, as most of the flux contributing to ML comes from a region extending up to $\sim 10r_g$ where the gravitational reddening has little impact. We argue that the observed value of ML is not expected to be lower than the intrinsic one by more than a few percent. The observed values of ML would be further decreased if the inclination is not face on — one should account for this fact before applying the method.

The last one is the model-dependence of our method. We assume the limited classical theory to describe the accretion flow. We neglect mass outflows, magnetic fields and apply the α prescription of viscosity with α independent of radius. These factors, especially the viscosity treatment, may have significant impact on ML vs OD/CD relation that we have obtained. Nayakshin et al. (2000) show that reproducing the light curves of GRS 1915+105 is possible only if much more complicated models are considered. Nevertheless, if the limit-cycle behavior is the actual reason of the observed variability of some microquasars, and if the extraction of ML and OD/CD parameters from the light curves is possible, then, under the limitations of our model, the BH spin can be roughly estimated, before other more accurate methods, such as fitting spectral energy distribution, are applied.

4.4. Evolution of the temperature-luminosity relation for the limit-cycle in classical theory

The maximal disk temperature-luminosity (T - L) correlation predicted by the classical theory of limit-cycles has been used to compare with observations (e.g. Gierliński & Done 2004; Kubota & Makishima 2004; Kubota et al. 2001). In Figure 6, we show the T - L evolution for the last cycle calculated in each model. The panels present the evolution for a given set of α and \dot{m} and different BH spins ($a^* = 0, 0.5$ and 0.95 marked by solid, dashed and dotted lines, respectively). These curves reveal several common features: (1) All of the cycles begin at the closely-located triangle points and spend a quarter of CD evolving along the curve in the anti-clockwise direction before they reach the square points, and finally spend the other 3/4 of CD to return to the starting location (triangles); (2) The evolution of all the cycles fits (with exception of the outbursts of the $a^* = 0.95$ case) between two straight lines corresponding to $L_{\text{disk}} \propto T_{\text{max}}^4$ relations with different color correction factors ($f_{\text{col}} = 1$ and 7.2 , see Gierliński & Done 2004); (3) The T - L curves of all the cycles are similar for most of CD except for the outburst state — the BH spin impact is revealed at the outburst of limit-cycle only; (4) During the mass restoring process (prior to the next outburst) the disk obeys $L_{\text{disk}} \propto T_{\text{max}}^{0.7}$ (see the dashed straight lines in all panels).

5. Discussion

The theory based on the standard viscosity prescription (1) predicts that radiation pressure-supported regions of radiatively efficient accretion disks are thermally and viscously unstable. The range of luminosity within which the disk is unstable is narrower for an (ad hoc) alternative viscosity prescription

$$\mathbb{T} = -\alpha \sqrt{P^{2-\mu} P_{\text{gas}}^\mu}, \quad (15)$$

where $0 \leq \mu \leq 1$ is a constant parameter (Szuszkiewicz 1990), with $\mu = 0$ corresponding to the standard prescription and $\mu = 1$ to the so-called “geometrical mean” prescription. The instability disappears for $\mu > 8/7$. A recent important work by Hirose et al. (2009) shows that the standard Shakura-Sunyaev viscosity prescription (1) fits their MHD simulations of accretion disks much better than the prescriptions (15) with $\mu > 0$. However, Hirose et al. (2009) also find that the radiation pressure supported MHD disks are thermally *stable* in their simulations (it is not known whether they are viscously stable). This result contradicts the hydrodynamical stability analysis. What are the MHD effects that stabilize the disk? One explanation is given in Hirose et al. (2009). They argue that although the viscosity prescription has the form (1), it should nevertheless be modified in a subtle way, because the “viscous heating” \mathbb{Q}^+ that occurs in the disk is *delayed* with respect to the MHD stress $\mathbb{T} = \mathbb{T}_{\text{MHD}}$,

$$\mathbb{Q}^+(t) = \mathbb{T}(t - \Delta t) \left[\frac{d\Omega}{dr} \right]. \quad (16)$$

Here Δt is the delay, found to be about 10 dynamical times, and Ω is the angular velocity of matter. It should be obvious that this modification is irrelevant in the stationary case. In an exhaustive *Newtonian* analytical stability analysis (Ciesielski et al. (2011), see also Lin et al. (2011)), parallel to the numerical work described in the present paper, we have confirmed (in general) that in some parameter space the suggestion made in Hirose et al. (2009) does stabilize the radiation pressure thermal instability. However, we also found a variety of different parameter ranges with interesting, and complex, oscillatory behaviors that need to be further investigated. The present paper makes the first step into this direction, by investigating the standard case $\Delta t = 0$. We already numerically simulate a few representative cases with $\Delta t \neq 0$. Another explanation to the absence of the thermal instability is given by Zheng et al. (2011). They attribute the stability to the magnetic pressure in the accretion disk, which was neglected in the traditional hydrodynamical stability analysis. They show that if the magnetic pressure decreases with response to an

increase of temperature of the accretion flow, the threshold of accretion rate above which the disk becomes unstable increases significantly compared to the case of not considering the magnetic pressure. The physical reason is that in this case the dependence of turbulent dissipation heating on temperature becomes weaker.

On the observational front, spin of BHs in several galactic BH candidates have recently been measured by fitting the observed spectral energy distribution with the relativistic geometrically thin accretion disk model (Shafee et al. 2006; McClintock et al. 2006). Among these objects, GRS 1915+105 is the most special one. It is believed to have an extreme Kerr BH with the spin very close to $a^* = J/M^2 = 1$ (see McClintock et al. 2006). It is also the only object that exhibits the quasi-regular luminosity variations (Belloni et al. 1997; Nayakshin et al. 2000; Janiuk et al. 2002; Watarai & Mineshige 2003; Ohsuga 2006; Kawata et al. 2006; Janiuk & Czerny 2011), similar to the limit-cycle predicted by the standard *Newtonian*, hydrodynamical models. Several questions need to be investigated here. May one explain the luminosity variations observed in GRS 1915+105 as the classic “slim-disk” limit-cycle behavior? What is the role of the nearly extreme spin of GRS 1915+105 in the context of the observed variability? Could the case of GRS 1915+105 help to find the answer about the proper viscosity prescription?

Our research shows that the shape of light curves weakly depend on BH spin. The only quantity that feels the impact of the BH spin is the maximal luminosity. Therefore, under the assumptions adopted in this paper (e.g., a constant α), the limit cycle can produce light curves which are only qualitatively similar to those observed in GRS1915+105, independent of BH spin. To obtain better agreement one has to construct more complicated models (e.g., Nayakshin et al. 2000). We prove that the cycle duration weakly depends on the BH spin. Thus, the observed value for GRS1915+105 most probably results from combined effects of viscosity and mass-supply rate and is not affected by the BH spin. The very presence of

limit cycle variability only in this object, if it is true, may challenge the explanation given by Hirose et al. (2009), but could be understood in the model of Zheng et al. (2011) as due to the high luminosity of this source compared to other sources.

6. Summary and conclusions

This paper is a sequel of Paper I (Li et al. 2007). We have changed the framework of study from the previous pseudo-Newtonian hydrodynamics to relativistic one. We have established the time-dependent basic equations for slim disk accretion in the full general relativity (Appendix A). We continue to use the *adaptive pseudospectral domain decomposition* method, which has been validated in Paper I, to solve these new equations. Our main results and conclusions are summarized as follows.

1. We have calculated two models assuming $\alpha = 0.07$ and $\dot{m} = 0.02$ and two values of BH spin. We find that the model with a non-spinning BH ($a^* = 0$) can stay in the steady state, but the model with a high-spinning BH ($a^* = 0.95$) undergo an outburst immediately after the beginning of the computation. These features agree with the predictions of the classical local analysis of stability (see Figure 1), thus the ability of the new relativistic code for distinguishing the thermally stable and unstable disks is validated, and it is confirmed that the BH spin can change the thermal stability of an accretion disk.

2. Following the time-evolution of twelve models we have explored the effects of BH spin on the limit-cycle behavior. We define four characteristic quantities to describe the limit-cycle behavior: the outburst duration (OD), cycle duration (CD), ratio of OD to CD, and maximal luminosity (ML). We find that the effects of BH spin on the quantities that depend on the disk structure at a wide range of radii (OD, CD and OD/CD), are easily disturbed and even obscured by the combined effects of viscosity and mass-supply.

However, ML is an exception. As it depends on the radiation coming from the inner region of the disk, it overcomes the impact of viscosity and mass-supply and reveals a monotonous positive dependence on BH spin.

3. We have discussed the possibility of using the OD/CD-ML diagram to estimate the BH spin. The advantage of this method is its simplicity, but the dispersion related to the unknown viscosity and mass-supply, as well as its model dependence limit its application. We suggest that one can use the OD/CD-ML relation to perform rapid and rough estimation, before more accurate BH spin estimations based on other methods are available.

4. We have presented and discussed the evolution of the T - L relation for limit-cycles with different model parameters, proving that BH spin changes the disk evolution only during the outburst phase.

We thank Feng Yuan for beneficial discussion. This work was supported by 973 Program under grant 2009CB824800, the National Natural Science Foundation of China under grants 10833002 and 11003016, the Natural Science Foundation of Fujian Province of China under grant 2010J01017, and by Polish Ministry of Science grants N203 0093/1466, N203 304035, N203 380336 and N203 381436.

A. Derivation of basic equations

The basic equations used in our paper, which make exploring the time-dependent behavior of accretion disks around Kerr BHs possible, are derived basing on Abramowicz et al. (1996, 1997), Gammie & Popham (1998) and Sądowski (2009). In this appendix, we give all of the derivation details that are ignored in the main part of our paper.

A.1. Metric and four-velocity

We use the Boyer-Lindquist spherical coordinates t, r, θ, ϕ to describe the Kerr BH metric. We use its reduced form near the equatorial plane, because the disk equations involve vertically averaged quantities and the disks we deal with are not very thick. The nonvanishing covariant and contravariant components of the reduced metric can be written as,

$$g_{tt} = -\frac{r-2M}{r}, \quad g_{t\phi} = -\frac{2Ma}{r}, \quad g_{\phi\phi} = \frac{A}{r^2}, \quad g_{rr} = \frac{r^2}{\Delta}, \quad g_{\theta\theta} = r^2; \quad (\text{A1})$$

and

$$g^{tt} = -\frac{A}{r^2\Delta}, \quad g^{t\phi} = -\frac{2Ma}{r\Delta}, \quad g^{\phi\phi} = \frac{r-2M}{r\Delta}, \quad g^{rr} = \frac{\Delta}{r^2}, \quad g^{\theta\theta} = \frac{1}{r^2}. \quad (\text{A2})$$

Where M and a are the mass and specific angular momentum of the BH respectively, $\Delta \equiv r^2 - 2Mr + a^2$, $A \equiv r^4 + r^2a^2 + 2Mra^2$. The metric is in the geometrical units ($c = G = 1$) and its signature is $(-+++)$.

The stress-energy tensor reads,

$$T^{ik} = \rho u^i u^k + p g^{ik} + s^{ik} + u^k q^i + u^i q^k, \quad (\text{A3})$$

where ρ , u^i , p , s^{ik} and q^i are the rest mass density, contravariant components of four-velocity, total pressure (the sum of the gas and radiation pressure), viscous stress tensor, and radiative energy flux, respectively.

The general form of the four-velocity is,

$$u^i = \gamma (e_{(t)}^i + V^{(r)} e_{(r)}^i + V^{(\phi)} e_{(\phi)}^i + V^{(\theta)} e_{(\theta)}^i), \quad (\text{A4})$$

where γ is the Lorentz factor, $V^{(j)}$ are velocities as measured in the Local Non Rotating Frame (LNRF) and $e_{(j)}$ are LNRF basis vectors. Near the equatorial plane, they take the following forms,

$$\gamma^{-2} = 1 - (V^{(r)})^2 - (V^{(\phi)})^2; \quad (\text{A5})$$

$$V^{(r)} = \frac{1}{\gamma} \frac{V}{\sqrt{1-V^2}}, \quad (\text{A6a})$$

$$V^{(\theta)} = U \cos \theta, \quad (\text{A6b})$$

$$V^{(\phi)} = \frac{1}{\gamma} \frac{\mathcal{L}r}{A^{1/2}}; \quad (\text{A6c})$$

and

$$e_{(t)} = \frac{A^{1/2}}{r\Delta^{1/2}} \frac{\partial}{\partial t} + \frac{2Ma}{A^{1/2}\Delta^{1/2}} \frac{\partial}{\partial \phi}, \quad (\text{A7a})$$

$$e_{(r)} = \frac{\Delta^{1/2}}{r} \frac{\partial}{\partial r}, \quad (\text{A7b})$$

$$e_{(\theta)} = \frac{1}{r} \frac{\partial}{\partial \theta}, \quad (\text{A7c})$$

$$e_{(\phi)} = \frac{r}{A^{1/2}} \frac{\partial}{\partial \phi}, \quad (\text{A7d})$$

where we have followed Bardeen et al. (1972) to use the relations (A7a)-(A7d), and we have introduced the radial velocity measured in the corotating frame (CRF) V , the vertical velocity parameter U and the angular momentum per unit mass $\mathcal{L}(\equiv u_\phi)$ to describe accretion flows.

According to equations (A6), (A7) and (A4), the contravariant components of the four-velocity in terms of V , U and \mathcal{L} are

$$u^t = \gamma \frac{A^{1/2}}{r\Delta^{1/2}}, \quad (\text{A8a})$$

$$u^r = \frac{V}{\sqrt{1-V^2}} \frac{\Delta^{1/2}}{r}, \quad (\text{A8b})$$

$$u^\phi = \frac{\mathcal{L}r^2}{A} + \gamma\omega \frac{A^{1/2}}{r\Delta^{1/2}}, \quad (\text{A8c})$$

$$u^\theta = \frac{\gamma}{r} U \cos \theta. \quad (\text{A8d})$$

The relevant covariant components are

$$u_t = -\gamma \frac{r\Delta^{1/2}}{A^{1/2}} - \omega\mathcal{L}, \quad (\text{A9a})$$

$$u_r = \frac{r}{\Delta^{1/2}} \frac{V}{\sqrt{1-V^2}}, \quad (\text{A9b})$$

$$u_\phi = \mathcal{L}, \quad (\text{A9c})$$

$$u_\theta = \gamma r U \cos \theta. \quad (\text{A9d})$$

At last, according to equation (A5), the Lorentz factor can be written as,

$$\gamma^2 = \frac{1}{1-V^2} + \frac{\mathcal{L}^2 r^2}{A}. \quad (\text{A10})$$

A.2. Mass conservation

The general form of the continuity equation is

$$\nabla_i(\rho u^i) = 0. \quad (\text{A11})$$

After vertical integration it takes the following form

$$u^t \frac{\partial \Sigma}{\partial t} = -\frac{1}{r} \frac{\partial}{\partial r} (\Sigma r u^r) - \Sigma \frac{\partial u^t}{\partial t}, \quad (\text{A12})$$

where Σ is the surface density. Substituting u^t and u^r with relations (A8a) and (A8b), we have

$$\frac{\partial \Sigma}{\partial t} = -\frac{r \Delta^{1/2}}{\gamma A^{1/2}} \left[\Sigma \frac{\partial u^t}{\partial t} + \frac{1}{r} \frac{\partial}{\partial r} \left(r \Sigma \frac{V}{\sqrt{1-V^2}} \frac{\Delta^{1/2}}{r} \right) \right], \quad (\text{A13})$$

where the time derivative $\frac{\partial u^t}{\partial t}$ can be substituted with the equation

$$\frac{\partial u^t}{\partial t} = \frac{A^{1/2}}{r \Delta^{1/2}} \frac{1}{\gamma} \left[\frac{V}{(1-V^2)^2} \frac{\partial V}{\partial t} + \frac{\mathcal{L} r^2}{A} \frac{\partial \mathcal{L}}{\partial t} \right], \quad (\text{A14})$$

which is obtained by operating time derivative on equation (A8a). In the right-hand-side of the above equation, there still exist two time derivatives $\frac{\partial V}{\partial t}$ and $\frac{\partial \mathcal{L}}{\partial t}$, but they can be evaluated before the evaluation of $\frac{\partial u^t}{\partial t}$ with equations (A18) and (A23).

A.3. Radial momentum conservation

The radial momentum conservation is expressed as the vanishing of the r -component of the divergence of the stress-energy tensor

$$\nabla_i T^{ir} = 0. \quad (\text{A15})$$

Expanding it

$$\begin{aligned} u^i \nabla_i u^r + \frac{1}{\rho} g^{rr} \frac{\partial p}{\partial r} &= 0 \\ \Rightarrow u^t \frac{\partial u^r}{\partial t} + u^r \frac{\partial u^r}{\partial r} + u^i \Gamma_{ki}^r u^k &= -\frac{1}{\rho} g^{rr} \frac{\partial p}{\partial r}, \end{aligned} \quad (\text{A16})$$

and then neglecting terms proportional to $\cos^2 \theta$ we get

$$u^t \frac{\partial u^r}{\partial t} + u^r \frac{\partial u^r}{\partial r} + \Gamma_{tt}^r u^t u^t + 2\Gamma_{t\phi}^r u^t u^\phi + \Gamma_{rr}^r u^r u^r + \Gamma_{\phi\phi}^r u^\phi u^\phi = -\frac{1}{\rho} g^{rr} \frac{\partial p}{\partial r}. \quad (\text{A17})$$

This equation can be reformulated as

$$\frac{\partial V}{\partial t} = \frac{\sqrt{1-V^2} \Delta}{\gamma A^{1/2}} \left[-\frac{V}{1-V^2} \frac{\partial V}{\partial r} + \frac{\mathcal{A}}{r} - \frac{1-V^2}{\rho} \frac{\partial p}{\partial r} \right], \quad (\text{A18})$$

where \mathcal{A} , Ω , Ω_{K}^+ , Ω_{K}^- , $\tilde{\Omega}$ and \tilde{R} are defined as in Abramowicz et al. (1996)

$$\mathcal{A} \equiv -\frac{MA}{r^3 \Delta \Omega_{\text{K}}^+ \Omega_{\text{K}}^-} \frac{(\Omega - \Omega_{\text{K}}^+)(\Omega - \Omega_{\text{K}}^-)}{1 - \tilde{\Omega}^2 \tilde{R}^2}, \quad (\text{A19a})$$

$$\Omega \equiv \frac{u^\phi}{u^t} = \frac{2Mar}{A} + \frac{r^3 \Delta^{1/2} \mathcal{L}}{\gamma A^{3/2}}, \quad (\text{A19b})$$

$$\Omega_{\text{K}}^\pm \equiv \pm \frac{M^{1/2}}{r^{3/2} \pm aM^{1/2}}, \quad (\text{A19c})$$

$$\tilde{\Omega} \equiv \Omega - \frac{2Mar}{A}, \quad (\text{A19d})$$

$$\tilde{R} \equiv \frac{A}{r^2 \Delta^{1/2}}. \quad (\text{A19e})$$

We have neglected the radial components of the viscous stress tensor (s^{ir}) as they are negligible for vertically integrated models of accretion disks.

A.4. Angular momentum conservation

The angular momentum conservation can be written as

$$\nabla_i(T_k^i \xi^k) = 0, \quad (\text{A20})$$

where $\xi^k (\equiv \delta_{(\phi)}^k)$ is the azimuthal Killing vector. After vertical integration we get

$$\Sigma \left(u^t \frac{\partial u_\phi}{\partial t} + u^r \frac{\partial u_\phi}{\partial r} \right) + \nabla_i(S_\phi^i) = 0, \quad (\text{A21})$$

where S_ϕ^i is the vertically integrated (i, ϕ) component of the viscous stress tensor. We follow Lasota (1994) to assume that the only nonvanishing component of S_ϕ^i is

$$S_\phi^r = -\nu \Sigma \frac{A^{3/2} \Delta^{1/2} \gamma^3}{r^5} \frac{\partial \Omega}{\partial r}, \quad (\text{A22})$$

where ν is the kinetic viscosity coefficient and Ω is the angular velocity with respect to the stationary observer [see definition (A19b)]. Finally, introducing \mathcal{L} and V with the equations (A8a), (A8b) and (A9c) we get

$$\frac{\partial \mathcal{L}}{\partial t} = -\frac{V \Delta}{\gamma \sqrt{1 - V^2} A^{1/2}} \frac{\partial \mathcal{L}}{\partial r} + \frac{\Delta^{1/2}}{\gamma \Sigma A^{1/2}} \frac{\partial}{\partial r} \left(\frac{\nu \Sigma A^{3/2} \Delta^{1/2} \gamma^3}{r^4} \frac{\partial \Omega}{\partial r} \right). \quad (\text{A23})$$

A.5. Half thickness evolution

Let us consider the vertical acceleration of the disk surface in the Zero Angular Momentum Observer (ZAMO) system of coordinates. The disk surface is defined in cylindrical coordinates as

$$z = H(r, t) \quad (\text{A24})$$

Therefore, the infinitesimal shift in the vertical direction can be expressed in the following way

$$dz = \frac{\partial H}{\partial r} dr + \frac{\partial H}{\partial t} dt. \quad (\text{A25})$$

Dividing both sides by dt we get

$$\frac{dz}{dt} = -V^{(\theta)} = \frac{\partial H}{\partial r} V^{(r)} + \frac{\partial H}{\partial t}. \quad (\text{A26})$$

Introducing U and V with the equations (A6a) and (A6b) we obtain

$$\frac{\partial H}{\partial t} = -U \cos \Theta_H - \frac{1}{\gamma} \frac{V}{\sqrt{1-V^2}} \frac{\partial H}{\partial r}, \quad (\text{A27})$$

where Θ_H is the colatitude angle corresponding to the disk surface ($\theta = \Theta_H$ and $H = r \cos \Theta_H$) at a certain radius.

A.6. Surface vertical motion

We follow Abramowicz et al. (1997) to assume the form of vertically integrated pressure as

$$P(r, \theta, t) = P_0(r, t) \left[1 - \frac{\cos^2 \theta}{\cos^2 \Theta_H} \right]. \quad (\text{A28})$$

Let us consider the θ -component of the divergence of stress-energy tensor

$$\nabla_k T_\theta^k = 0. \quad (\text{A29})$$

Expanding and vertically integrating we get

$$\frac{1}{\Sigma} \frac{\partial P}{\partial \theta} = -u^k u_{\theta,k} + \Gamma_{\theta k}^i u_i u^k. \quad (\text{A30})$$

From equation (A28) it follows that

$$\left. \frac{\partial P}{\partial \theta} \right|_{\theta=\Theta_H} = \frac{2P}{\cos \Theta_H}. \quad (\text{A31})$$

Taking both relations into account we have

$$\frac{\partial U}{\partial t} = \frac{\Delta^{1/2}}{\gamma^2 A^{1/2} \cos \Theta_H} \mathcal{R} - \frac{U}{\gamma^2} \left(\frac{V}{(1-V^2)^2} \frac{\partial V}{\partial t} + \frac{\mathcal{L} r^2}{A} \frac{\partial \mathcal{L}}{\partial t} \right) - \frac{U}{H} \frac{\partial H}{\partial t}, \quad (\text{A32})$$

where

$$\mathcal{R} \equiv -\frac{2P}{\Sigma \cos \Theta_H} + (\mathcal{L}^2 - a^2(u_t u_t - 1)) \frac{\cos \Theta_H}{r^2} - u^r \frac{\partial u_\theta}{\partial r}, \quad (\text{A33a})$$

$$u_t u_t = \left[\gamma \frac{r \Delta^{1/2}}{A^{1/2}} + \omega \mathcal{L} \right]^2, \quad (\text{A33b})$$

$$u^r \frac{\partial u_\theta}{\partial r} = \frac{V \Delta^{1/2}}{r \sqrt{1 - V^2}} \frac{\partial}{\partial r} (\gamma U_r \cos \Theta_H). \quad (\text{A33c})$$

A.7. The energy conservation

From the general form of the energy conservation equation

$$\nabla_i (T^{ik} \eta_k) = 0, \quad (\text{A34})$$

we obtain, in the non-relativistic fluid approximation,

$$\rho \left[u^t \frac{\partial \epsilon}{\partial t} + u^r \frac{\partial \epsilon}{\partial r} \right] + \nabla_i (\eta \sigma^{it}) + \nabla_i (u^t q^i + u^i q^t) = 0. \quad (\text{A35})$$

Similarly like in Landau & Lifshitz (1959) (their Eq. 49.4), after vertical integration, it can be reformulated as

$$\Sigma T \left[u^t \frac{\partial S}{\partial t} + u^r \frac{\partial S}{\partial r} \right] = F^+ - F^-. \quad (\text{A36})$$

Where S is the entropy per unit mass, F^+ is the local viscous heat generation rate and F^- is the radiative cooling rate (see Abramowicz et al. (1996))

$$F^+ = \nu \gamma^4 \Sigma \frac{A^2}{r^6} \left(\frac{\partial \Omega}{\partial r} \right)^2, \quad (\text{A37})$$

$$F^- = \frac{8\sigma T^4}{3\tau_R/2 + \sqrt{3} + 1/\tau_P}. \quad (\text{A38})$$

Thermodynamical relations give (for $p = p_{\text{rad}} + p_{\text{gas}}$)

$$T \frac{\partial S}{\partial r} = c_V T \left(\frac{1}{T} \frac{\partial T}{\partial r} - (\Gamma_3 - 1) \frac{1}{\rho} \frac{\partial \rho}{\partial r} \right), \quad (\text{A39})$$

$$T \frac{\partial S}{\partial t} = c_V T \left(\frac{1}{T} \frac{\partial T}{\partial t} - (\Gamma_3 - 1) \frac{1}{\rho} \frac{\partial \rho}{\partial t} \right). \quad (\text{A40})$$

The appropriate sum of the derivatives of ρ can be substituted using the continuity equation

$$u^t \frac{1}{\rho} \frac{\partial \rho}{\partial t} + u^r \frac{1}{\rho} \frac{\partial \rho}{\partial r} \approx - \frac{\partial u^t}{\partial t} - \frac{1}{r^2} \frac{\partial}{\partial r} (r^2 u^r) + \frac{U}{r}. \quad (\text{A41})$$

Taking all together we get

$$c_V \left[\Sigma \left(u^t \frac{\partial T}{\partial t} + u^r \frac{\partial T}{\partial r} \right) - (\Gamma_3 - 1) T \Sigma \left(- \frac{\partial u^t}{\partial t} - \frac{1}{r^2} \frac{\partial}{\partial r} (r^2 u^r) \right) \right] = F^+ - F^-, \quad (\text{A42})$$

where

$$c_V = \frac{4 - 3\beta}{\Gamma_3 - 1} \frac{P}{\Sigma T}, \quad (\text{A43a})$$

$$\Gamma_3 - 1 = \frac{(4 - 3\beta)(\gamma_{\text{gas}} - 1)}{12(1 - \beta)(\gamma_{\text{gas}} - 1) + \beta}, \quad (\text{A43b})$$

$$\beta = \frac{p_{\text{gas}}}{p}. \quad (\text{A43c})$$

Ultimately we get

$$\frac{\partial T}{\partial t} = \frac{1}{\Sigma} \frac{r \Delta^{1/2}}{\gamma A^{1/2}} \left[\frac{F^+ - F^-}{c_V} + (\Gamma_3 - 1) T \Sigma \left(- \frac{\partial u^t}{\partial t} - \frac{1}{r^2} \frac{\partial}{\partial r} (r^2 u^r) \right) \right] - \frac{V \Delta}{\gamma \sqrt{1 - V^2} A^{1/2}} \frac{\partial T}{\partial r}. \quad (\text{A44})$$

REFERENCES

- Abramowicz, M. A., Czerny, B., Lasota, J.-P., Szuszkiewicz, E. 1988, *ApJ*, 332, 646
- Abramowicz, M. A., Chen, X.-M., Granath, M. & Lasota J.-P. 1996, *ApJ*, 471, 762
- Abramowicz, M. A., Lanza, A., & Percival, M. J. 1997, *ApJ*, 479, 179
- Bardeen, J. M., Press, W. H., & Teukolsky, S. A. 1972, *ApJ*, 178, 347
- Belloni, T., Mendez, M., King, A. R., van der Klis, M., & van Paradijs, J. 1997, *ApJ*, 488, L109
- Ciesielski, A., Wielgus, M., Sądowski, A., Abramowicz, M. A., Lasota, J.-P., Kluźniak W., 2011, in preparation
- Cunningham, C. T., & Bardeen, J. M., 1973, *ApJ*, 183, 237
- Fanton, C., Calvani, M., Felice F., & Čadež A., 1997, *PASJ*, 49, 159
- Gammie, C. F., & Popham, R. 1998, *ApJ*, 498, 313
- Gierliński, M., & Done, C. 2004, *MNRAS*, 347, 885
- Hirose, S., Krolik, J. H., & Blaes, O. 2009, *ApJ*, 691, 16
- Honma, F., Matsumoto, R., & Kato, S. 1991, *PASJ*, 43, 147
- Janiuk, A., Czerny, B., & Siemiginowska, A. 2002, *ApJ*, 576, 908
- Janiuk, A., & Czerny, B. 2011, *MNRAS*, submitted
- Kato, S., Fukue, J., & Mineshige, S. 1998, *Black-Hole Accretion Disks* (Kyoto: Kyoto Univ. Press)
- Kawata, A., Watarai, K., & Fukue, J. 2006, *PASJ*, 58, 477

- Kubota A., & Makishima K. 2004, ApJ, 601, 428
- Kubota A., Makishima K., & Ebisawa K. 2001, ApJ, 560, L147
- Landau, L. D., Lifshitz, E. M. 1959, Fluid mechanics. Course of theoretical physics (Oxford: Pergamon Press)
- Lasota, J. P. 1994, in NATO ASIC Proc. 417: Theory of Accretion disks 2, ed. W. J. Duschl, J. Frank, F. Meyer, E. Meyer-Hofmeister, & W. M. Tscharnuter, (Dordrecht: Kluwer), 341
- Lasota, J.-P., Pelat, D. 1991, A&A, 249, 574
- Li, S.-L., Xue, L. & Lu, J.-F. 2007, ApJ, 666, 368(Paper I)
- Lin, D.-B., Gu, W.-M., & Lu, J.-F. 2011, MNRAS, in press (arXiv:1104.0859)
- Mayer, M., & Pringle, J. E. 2006, MNRAS, 368, 379
- McClintock, J. E., Shafee, R., Narayan, R., Remillard, R. A., Davis, S. W., & Li, L.-X. 2006, ApJ, 652, 518
- Nayakshin, S., Rappaport, S., & Melia, F. 2000, ApJ, 535, 798
- Ohsuga, K. 2006, ApJ, 640, 923
- Papaloizou, J. & Szuszkiewicz, E. 1994, MNRAS, 268, 29
- Paczynski, B., & Wiita, P. J. 1980, A&A, 88, 23
- Śądowski, A. 2009, ApJS, 183, 171
- Śądowski, A., Abramowicz, M. A., Bursa, M., Kluźniak, W., Lasota, J.-P., Różańska, A. 2011, A&A, in press

- Shafee, R., McClintock, J. E., Narayan, R., Davis, S. W., Li, L.-X., & Remillard, R. A. 2006, *ApJ*, 636, L113
- Shakura, N. I., & Sunyaev, R. A. 1973, *A&A*, 24, 337
- Szuskiewicz, E. 1990, *MNRAS*, 244, 377
- Szuskiewicz, E., & Miller, J. C. 1997, *MNRAS*, 287, 165
- Szuskiewicz, E., & Miller, J. C. 1998, *MNRAS*, 298, 888
- Szuskiewicz, E. & Miller, J. C. 2001, *MNRAS*, 328, 36(SM01)
- Teresi, V., Molteni, D., & Toscano, E. 2004a, *MNRAS*, 348, 361
- Teresi, V., Molteni, D., & Toscano, E. 2004b, *MNRAS*, 351, 297
- Watarai, K., & Mineshige, S. 2003, *ApJ*, 596, 421
- Zheng, S.-M., Yuan, F., Gu, W.-M., & Lu, J.-F. 2011, *ApJ*, 732, 52

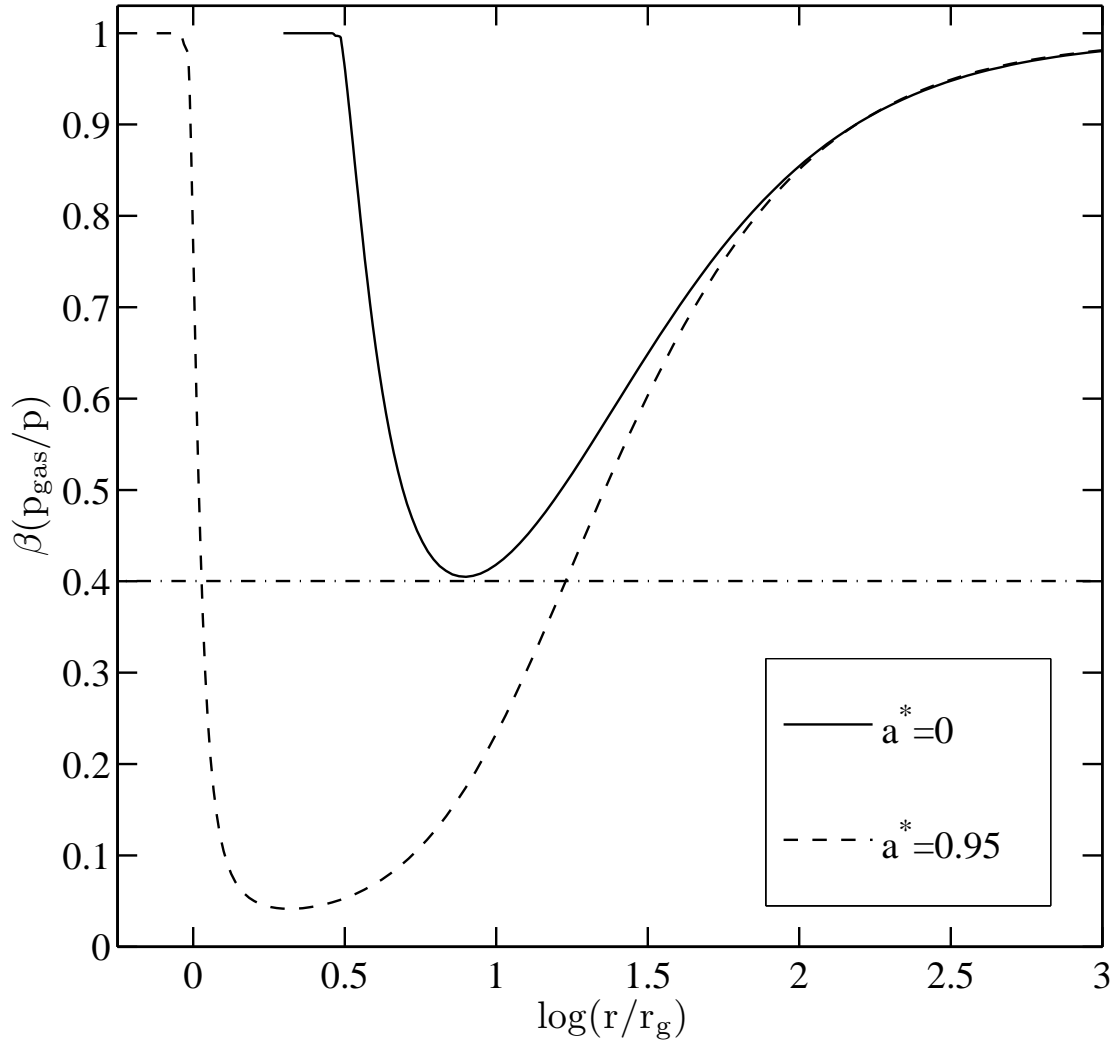


Fig. 1.— Profiles of ratio of gas pressure to total pressure. According to the local analysis of stability (e.g., Kato et al. 1998, p.155), the disk region with $\beta < 0.4$ is thermally unstable.

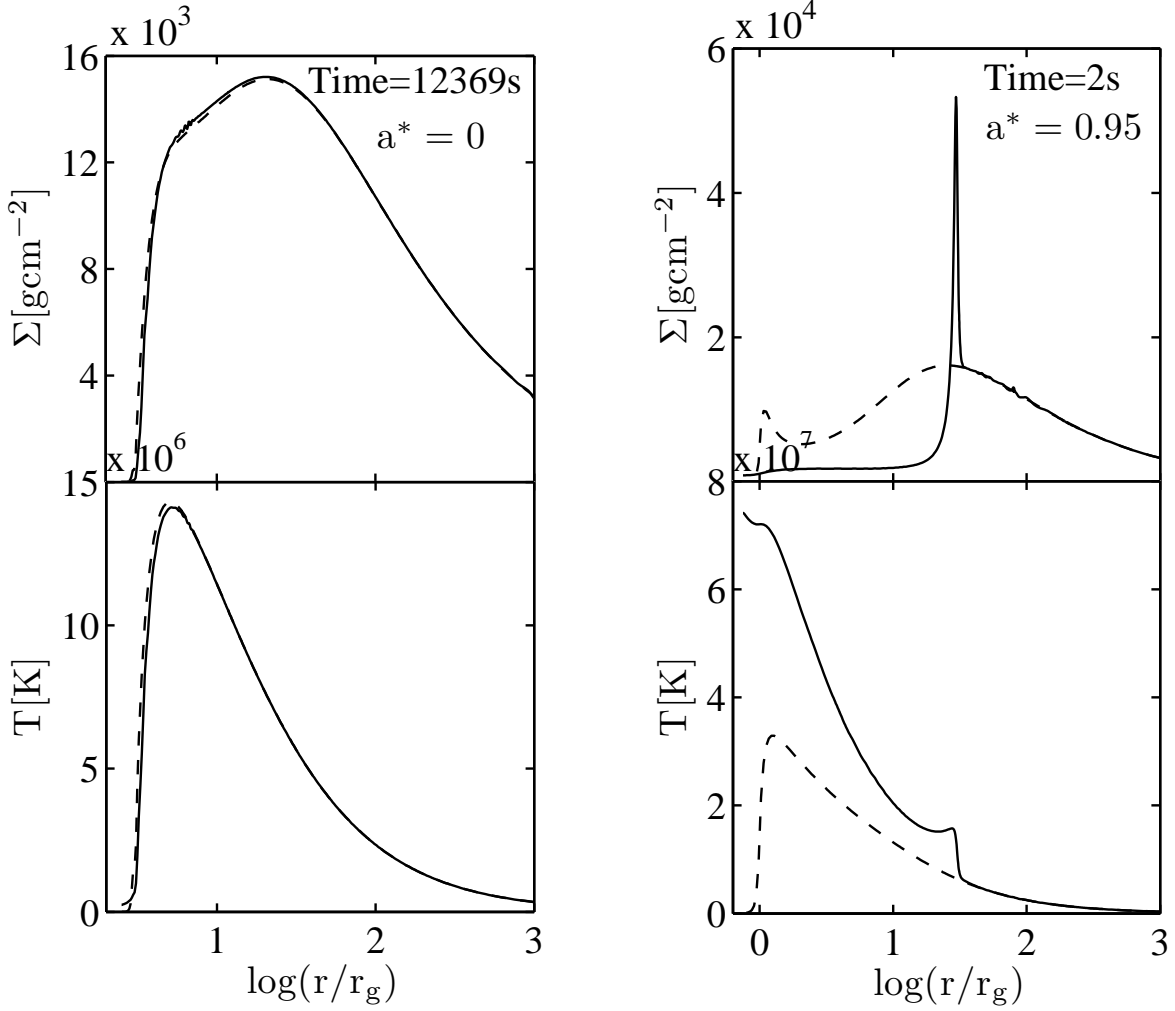


Fig. 2.— Profiles of surface density and temperature of two special cases. Dash lines correspond to the initial state, but solid lines are the relevant snapshots at the certain time.

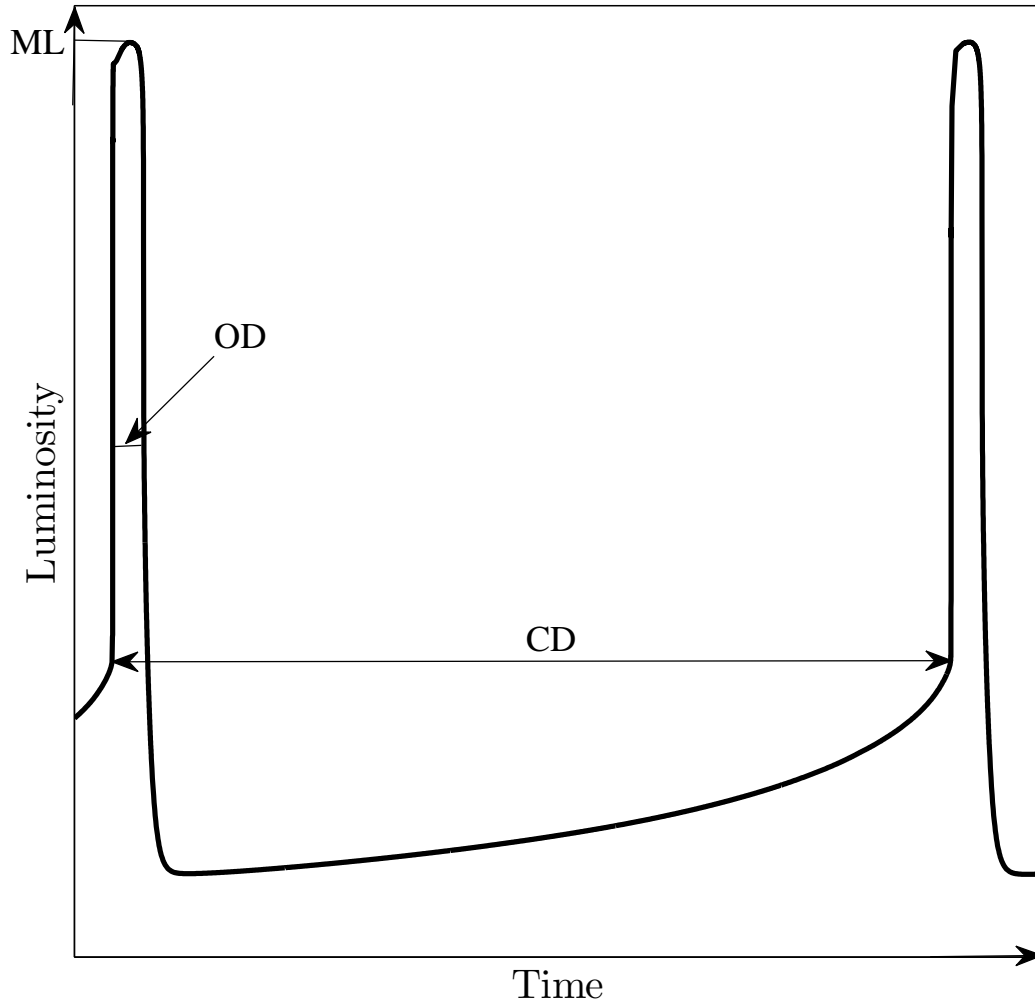


Fig. 3.— Sketch for explaining the definitions of characteristic quantities.

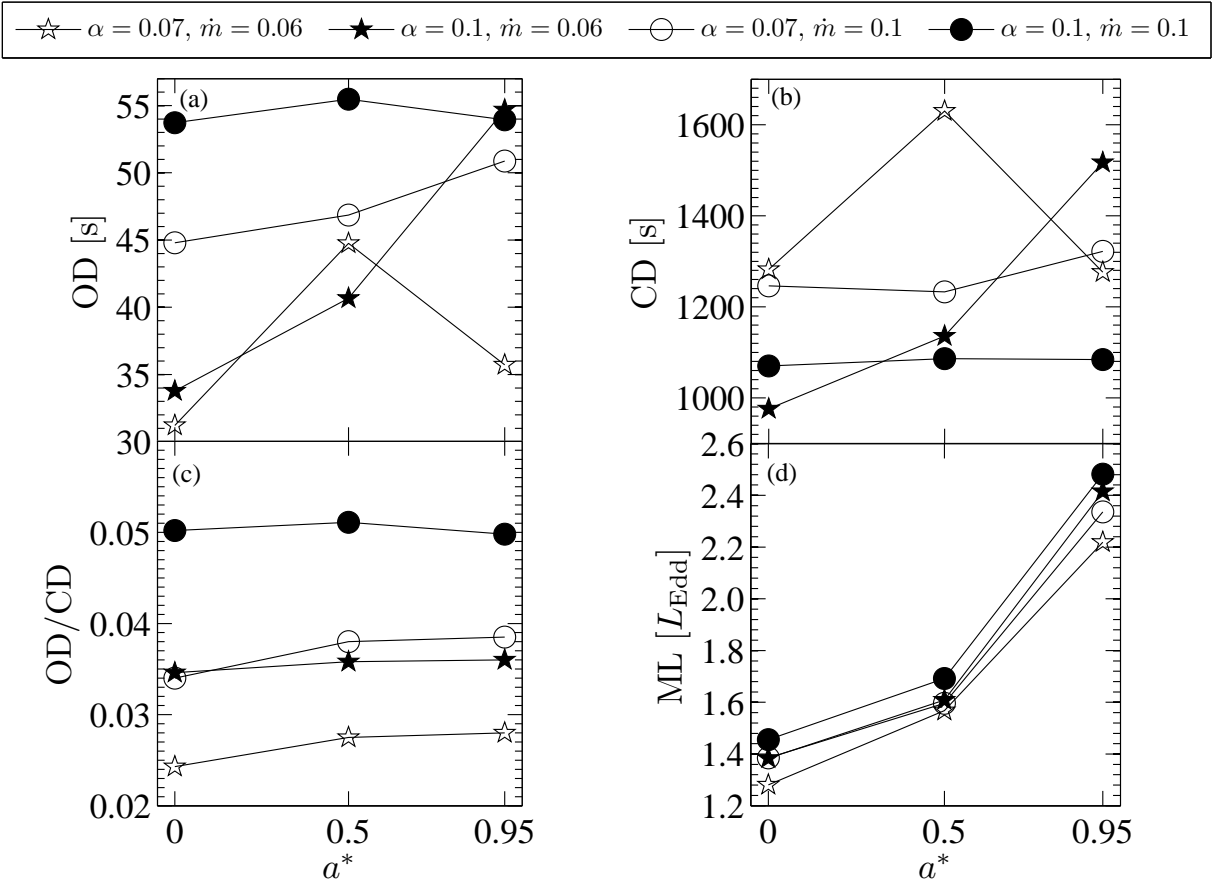


Fig. 4.— Correlation between the characteristic quantities and a^* .

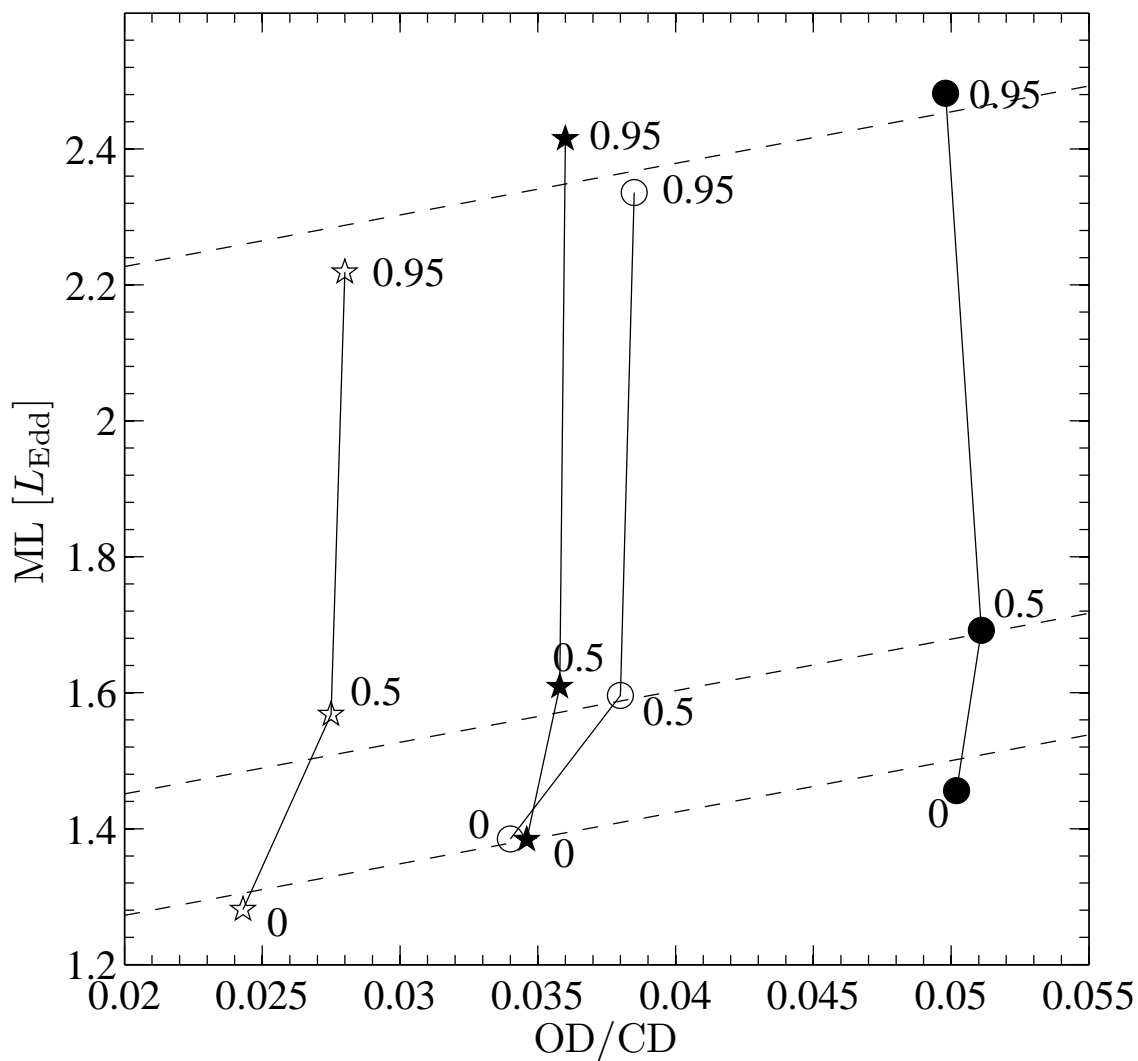


Fig. 5.— Plot of maximal luminosity versus ratio of OD to CD. The numbers near each data point are the values of a^* . The meanings of markers are the same as those in Figure 4. The dashed lines are the OD/CD-ML fitted lines for different a^* cases.

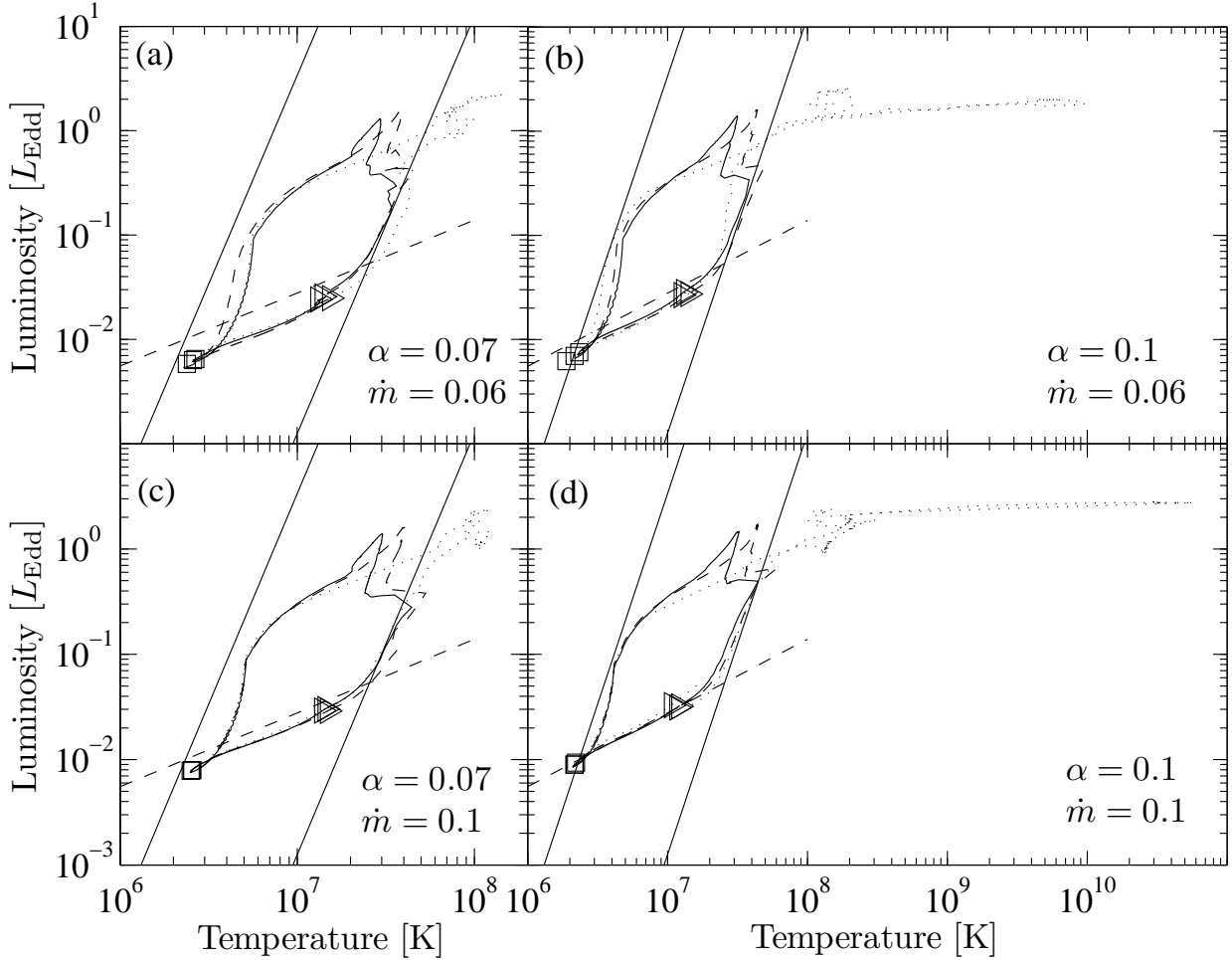


Fig. 6.— Evolution of the last cycle for the groups with different α and \dot{m} in the maximal disk temperature - luminosity (T - L) plane. All cycles begin at the triangle points, and then evolve along the curve in the anti-clockwise direction. The square points are used to denote the quarter of cycle durations. The solid straight lines in each panel represent $L_{\text{disk}} \propto T_{\text{max}}^4$ for a non-spinning BH (see eq. (3) of Gierliński & Done 2004). They are calculated with the color temperature correction $f_{\text{col}} = 1$ for the left lines and $f_{\text{col}} = 7.2$ for the right ones. The dashed straight lines denote the $L_{\text{disk}} \propto T_{\text{max}}^{0.7}$ relation. In each panel, the solid, dashed, and dotted curves are for the different BH spins with $a^* = 0, 0.5, 0.95$, respectively.

Table 1. Four limit-cycle characteristic quantities of the twelve cases¹

a^*	α	\dot{m}	OD [s]	CD [s]	OD/CD	ML [L_{Edd}]
0	0.07	0.06	31.21±0.12 (0.38%) ²	1282±3 (0.23%)	(2.43±0.02)×10 ⁻² (0.61%)	1.281±0.001 (0.07%)
0.5	0.07	0.06	44.76±0.32 (0.71%)	1630±4 (0.25%)	(2.75±0.03)×10 ⁻² (0.96%)	1.568±0.003 (0.17%)
0.95	0.07	0.06	35.72±0.14 (0.38%)	1276±10 (0.79%)	(2.80±0.04)×10 ⁻² (1.17%)	2.219±0.018 (0.79%)
0	0.1	0.06	33.78±0.12 (0.35%)	976±3 (0.31%)	(3.46±0.03)×10 ⁻² (0.66%)	1.384±0.003 (0.18%)
0.5	0.1	0.06	40.67±0.21 (0.50%)	1136±5 (0.44%)	(3.58±0.04)×10 ⁻² (0.94%)	1.609±0.003 (0.18%)
0.95	0.1	0.06	54.68±0.45 (0.81%)	1517±10 (0.66%)	(3.60±0.06)×10 ⁻² (1.47%)	2.415±0.008 (0.32%)
0	0.07	0.1	44.80±0.15 (0.33%)	1246±4 (0.33%)	(3.40±0.03)×10 ⁻² (0.66%)	1.385±0.002 (0.14%)
0.5	0.07	0.1	46.86±0.12 (0.24%)	1233±3 (0.25%)	(3.80±0.02)×10 ⁻² (0.49%)	1.596±0.003 (0.17%)
0.95	0.07	0.1	50.87±0.27 (0.52%)	1322±3 (0.23%)	(3.85±0.03)×10 ⁻² (0.75%)	2.336±0.006 (0.23%)
0	0.1	0.1	53.73±0.53 (0.98%)	1070±4 (0.38%)	(5.02±0.07)×10 ⁻² (1.36%)	1.456±0.002 (0.08%)
0.5	0.1	0.1	55.47±0.70 (1.25%)	1086±9 (0.83%)	(5.11±0.11)×10 ⁻² (2.08%)	1.692±0.003 (0.17%)
0.95	0.1	0.1	53.94±0.47 (0.87%)	1084±5 (0.47%)	(4.98±0.07)×10 ⁻² (1.34%)	2.482±0.004 (0.16%)

¹See §4 for the definitions of OD, CD, and ML.

²The values showed in the columns, OD, CD, OD/CD and ML are collected as "mean value"±"standard deviation" (relative deviation).